3-26-2020

Extracting Range Data From Images Using Focus Error

Erik M. Madden

Extracting Range Data from Images using Focus Error

THESIS

Erik M Madden, 2nd Lieutenant, USAF

AFIT-ENG-MS-20-M-037

DEPARTMENT OF THE AIR FORCE
AIR UNIVERSITY

AIR FORCE INSTITUTE OF TECHNOLOGY

Wright-Patterson Air Force Base, Ohio

AFIT-ENG-MS-20-M-037

Extracting Range Data from Images using Focus Error

THESIS

Presented to the Faculty

Department of Electrical and Computer Engineering

Graduate School of Engineering and Management

Air Force Institute of Technology

Air University

Air Education and Training Command

in Partial Fulfillment of the Requirements for the

Degree of Master of Science in Electrical Engineering

Erik M Madden, B.S.E.E.

2nd Lieutenant, USAF

March, 2020

AFIT-ENG-MS-20-M-037

Extracting Range Data from Images using Focus Error

THESIS

Erik M Madden, B.S.E.E.
2nd Lieutenant, USAF

Committee Membership:

Stephen C Cain, Ph.D
Chair

Maj David J Becker, Ph.D
Member

Col Brian J Neff, Ph.D
Member

Abstract

Air-to-air refueling (AAR) has become a staple when performing long missions with aircraft. With modern technology, however, people have began to research how to perform this task autonomously. Automated air-to-air refueling (A3R) is this exact concept. Combining many different systems, the idea is to allow computers on the aircraft to link up via the refueling boom, refuel, and detach before resuming pilot control. This document lays out one of the systems that is needed to perform A3R, namely, the system that extracts range data. While stereo cameras perform such tasks, there is interest in finding other ways of accomplishing the same mission.

This research uses focus error to extract the same range from an image that can be obtained from a stereo camera system. This document will discuss how far A3R has come as well as the benefits of a focus error method. A simulation of how this process can function will also be shown, and will include a processing algorithm for extracting range information. A laboratory experiment section is introduced, which describes how this research can be pursued in the future.

Table of Contents

Page

List of Figures

List of Tables

Extracting Range Data from Images using Focus Error

I. Introduction

This chapter will outline the flow of the document and include the background work. It will also describe the problem that will be addressed by this research as well as the goals.

1.1 Motivation

While two cameras are needed to measure the range to an object using stereo vision, this research will discuss how ranging could be accomplished with a single camera. This research will look into a different method for automated air-to-air refueling (A3R), specifically, finding range data through focus estimation. So far, the method of choice for completing this task uses two cameras at a fixed distance apart and calculates the range based on several factors from the images [2]. The research in this document, however, will use focus error in order to find the range to a target. As mentioned above, the end goal would be to use this method for more accurate and faster air-to-air refueling.

Collecting range data is essential in so many ways for the Air Force to carry out its mission successfully. There are a multitude of ideas that can be implemented in order to achieve this goal. Range data in this research will be collected and analyzed in the hopes of improving the Air Force's ability to accomplish automatic docking maneuvers for unmanned aircraft. The importance of this concept is to allow an unmanned aerial vehicle (UAV) the ability to connect to a refueling tanker even if

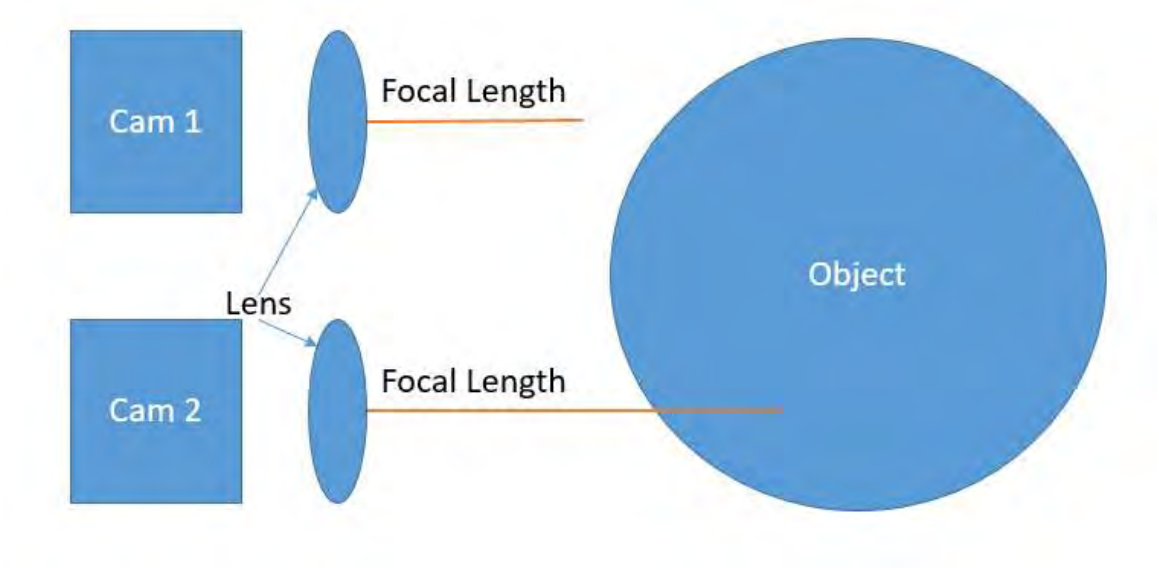

Figure 1: Setup of Two Cameras using Focus Error Method

the pilot looses control of the aircraft. The goal would be for the automatic flight control system to refuel, disconnect from the tanker and return control to the pilot.

Another idea that would benefit from this research would be if a pilot did lose control of the aircraft, the aircraft could automatically dock itself to another and get flown to a location where the pilot could regain control. The goals of this research are to expand on methods of finding range from photographs. This is done by analyzing the focus of the object in the image. While traditionally, two cameras are needed to do this, accomplishing that task with one would be a great achievement. The idea is to take a set of estimated ranges from a known window and have pictures at interval distances from the low estimated value to the highest one. These images are then compared to the image collected by the camera. The range estimate that produces the least amount of error through this comparison becomes the estimated range.

The reflectivity of the object would be a known quantity as a pattern could be placed on the refueling tanker in the form of a bar target or some other high contrast pattern. A brief setup of this research's overall concept can be seen in Figure 1.

1.2 Literature Review

1.2.1 Refueling the RPAs

Authors: Rebecca Grant

This document focuses on the general history of automated in flight refueling and how far it has come. Automated refueling started as a mere thought in the late 1990s with use of global positioning system (GPS). Maj Jeffery Stephenson stated that an aircraft would be able "to perform the mission of two or three unrefuelable UAVs [1]." This idea would reduce the cost of missions drastically. The problem came when dealing with having to connect the refueling hose to the UAV and requires far more fine-tuning than the autopilot systems are designed to achieve. Obtaining true autonomous refueling is quite difficult and requires aspects from many different systems to include robotics, telemetry, communications, electro-optics and so much more.

Organizations like the National Aeronautics and Space Administration (NASA) and Defense Advanced Research Projects Administration (DARPA) first demonstrated how to obtain range information from a fueling tanker through an air stream. This was the foundation to autonomously obtaining range data [1]. In 2006, there was a successful, nearly full autonomous mission between a tanker and an aircraft. The only drawback was that pilot consent was required at particular points in the research. Such aspects were expected seeing as how the idea of obtaining this data automatically was new.

The following year, in 2007, was when a full refueling demo was logged. The aircraft was reported to have the ability to "join the tanker from up to [2.3] miles behind, 1000 feet below, and 30 degrees off heading [1]." This feat was a huge accomplishment because of it being fully autonomous. The end goal was to have not only the UAV automated, but the boom to be as well. This, however was much more dif-

ficult. Other methods were attempted such as pattern recognition but failed because of low lighting and too much on board processing time required. Later, a method was chosen that would use optical recognition with the aid of algorithms. The end goal here, according to an AFRL official, was "to be able to fly something without a pilot in it within 40 feet of a manned vehicle.[1]"

Automatic in air refueling took a huge leap in 2007 when pilots only needed to take off and switch to the automated system. The jet ran through seven refueling positions. This included "contact, pre-contact, left and right inboard observation, left and right outboard observation, and breakaway [1]." This was a huge success because the aircraft stayed connected for 20 minutes and was controlled by the automated systems for 1 hour and 40 minutes in total.

Further research was desired and in 2010, Air Force Research Laboratory (AFRL)

awarded their contract to Boeing with hopes of them finding a way to apply this same concept to a long range bomber. Boeing came up with the concept of doing this using optical tracking with the key being able to steer the boom with an image placed on the remotely piloted aircraft (RPA)[1]. Future work on these systems includes applying it to an entire fleet in order to have minimal pilots in harm's way.

1.2.2 Improve a 3D distance measurement accuracy in stereo vision systems using optimization methods' approach

Authors: J.C Rodriguez-Quinonez, O. Sergiyenko, W. Flores-Fuentes, M. Rivas-Lopez, D. Hernandez-Balbuena, R. Rascon, P. Mercorelli

One of the methods already developed for obtaining range data is by use of stereo vision cameras. This is a process where two cameras are placed a fixed distance apart, both snap an image of the same scene and extract range data based on the connection between the two images. Another way of explaining this is that it is the process "of extracting 3-D information from multiple 2-D views of a scene [2]." As mentioned in an article by Rodriguez, a setup is shown in Figure 2 of how the cameras take the desired images [2]. With stereo cameras, the further apart they are, the better the results will be. From Figure 2, a is the distance between the two cameras, x_R, y_R are the right camera's coordinates, and x_L, y_L are the left camera's coordinates. Furthermore, angles B and C are the angles between the camera to the plane of the object and β is the angle of rise between the cameras and the object. Lastly, x, y, and z are the spacial location variables of the object. Given all of these variables and the use of the Law of Sines, x, y, and z are derived from Equations 1, 2, and 3 [2].

$$x = a * \frac{\sin(B)\sin(C)}{\sin(B+C)} \tag{1}$$

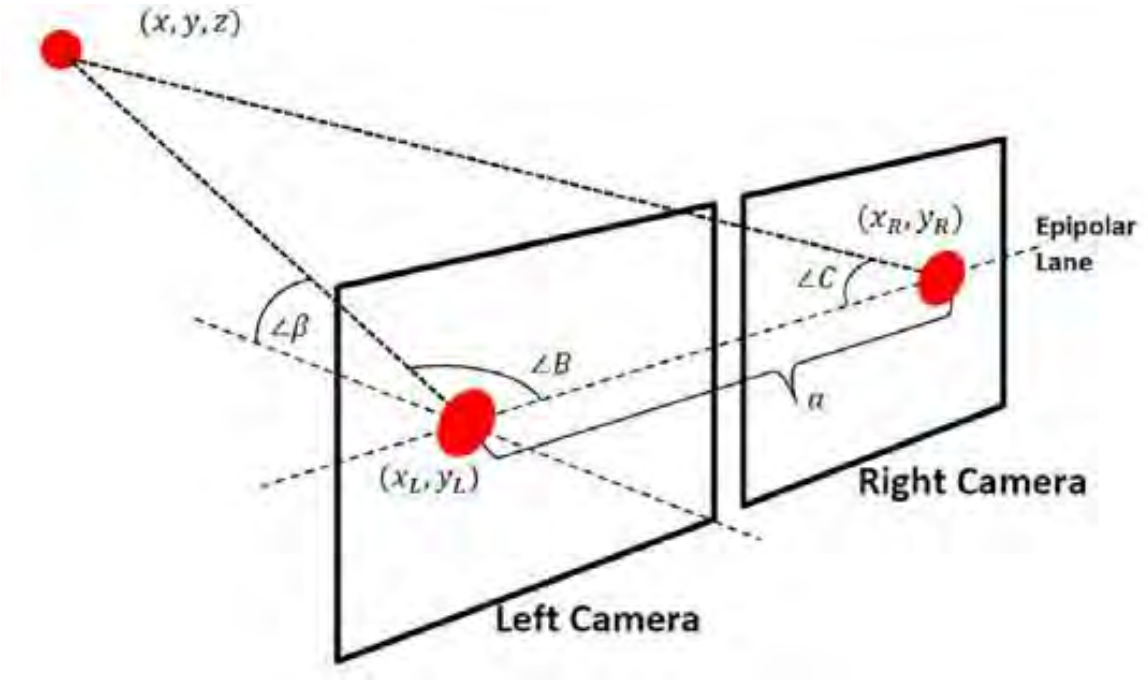

Figure 2: Stereo Cameras Setup Diagram

$$y = a\left(\frac{1}{2} - \frac{\sin(C)\cos(B)}{\sin(B+C)}\right) \tag{2}$$

$$z = a * \frac{\sin(C)\sin(B)\sin(\beta)}{\sin(B+C)} \tag{3}$$

Once the cameras get their different shots of the object, they can then process the input data and output an estimated range value. The process then looks at the intensity correlation in order to locate where the object is [2]. A setup of a pair of stereo cameras can be seen in Figure 3.

1.2.3 Considerations for a NATO Concept of Operations

Authors: Steve McLaughlin, Mark Pilling, Phillip Weber, Ba Nguyen

This document touched base mainly on how far research has come when describing air-to-air refueling (AAR). This document, which was published in 2019, mentions that while the automation of this idea has come a long way, it is not fully automated.

Figure 3: Stereo Cameras Setup

There are still checkpoints that need to be verified by a person when performing A3R but the individual tasks are automated. According to the document, concepts of operations, which are documents that describe how a system functions, need to be better understood, even with all the research performed up to this point[3]. The future of this project, according to the article, would be to have the task be completely automated. This would include receiving a word or message telling the aircraft it needs to refuel, which then can be accomplished without verification from a human pilot. A standard probe and drogue connection can be seen in Figure 4 [3].

Figure 4: Probe and Drogue Connection

1.3 Document Overview

This document's goal is to establish groundwork for obtaining range data by analyzing focus error from images. This document will be comprised of four other chapters. Chapter two will focus on a simulation for estimating range. This chapter discusses how the simulation was written, a breakdown of the code used and what it does to include how data is generated. There will also be error plots and description of how the error is calculated and why it's calculated the way it is(there are multiple ways to calculate the error for the simulation). Chapter three will focus on the data processing algorithm and how it was derived. This will also include a breakdown of the code used and descriptions of how the algorithm takes the data and outputs estimated range values. Chapter four will be comprised of the laboratory experiment. This will include how the data is entered, analyzed, and how range is reported from the algorithm. This chapter will also show error calculations using the measured laboratory data and explain its significance. The fifth chapter will be the conclusion. This chapter will wrap up the research as well as talk about a few different ways this

process can be improved and some other ideas of future research avenues.

II. Simulation Data

2.1 Preamble

This chapter will focus on the simulation aspect of the research. Matlab was used to produce a set of images that could be used as data in order to test the new algorithm. This section consists of an explanation of two programs. The first program is simply the main one that generates the data. The second program is used to generate the point spread function (PSF) for different range estimates to be used in the main program.

2.2 Simulation Summary

The first step to testing out the main idea of this research is to create a simulation where the algorithm could take simulated data and produce expected results. This would ensure that the algorithm was functioning as anticipated. This was completed by using Matlab and generating artificial data in order to come up with a suitable algorithm for accomplishing the goal of the research. In the simulation, the amount of pixels in the plane is set to 100 by 100($N = 100$) and the amount of background light is set to zero ($B = 0$). The range, in units of meters, is defined by Equation 4.

$$R(x, y) = 2.5 \tag{4}$$

In this equation, x and y are coordinates in the image plane and the range, R, is set to 2.5 meters at each point. Furthermore the center 20 pixels are defined by Equation 5.

$$R(x, y) = 2.1 \tag{5}$$

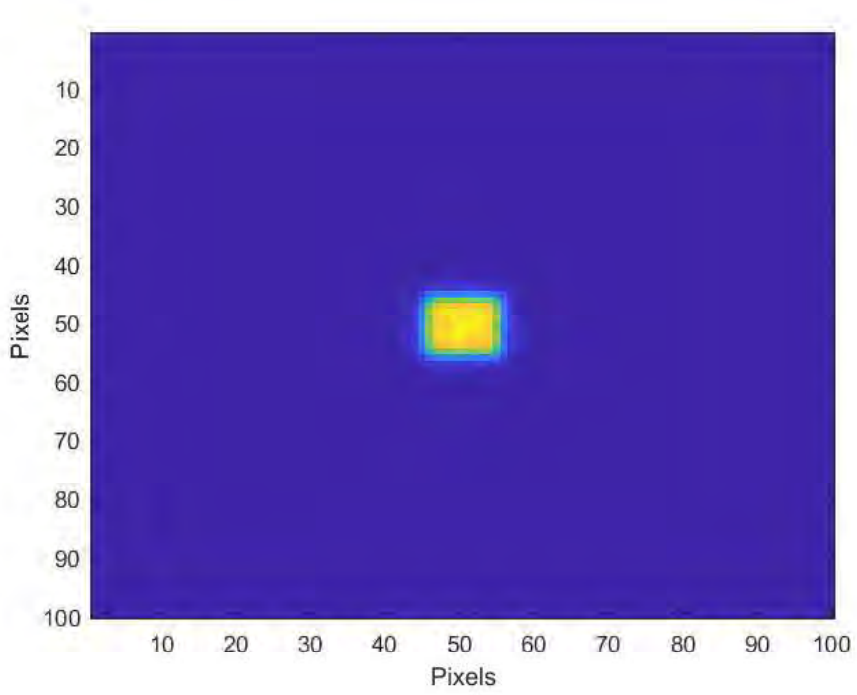

Figure 5: Camera A Output

When these two equations are ran through the simulation, the range image is formed. This image is illustrated in Figure 7 and the reflection of the image is defined in Equation 6, which illustrates the intensity, or reflectivity of the center 10 by 10 pixels. An illustration of the reflect matrix that was built can be viewed in Figure 8.

$$Reflect(x, y) = 1000 \tag{6}$$

A few parameters are then set. The diameter of the simulated lens is set to 10 centimeters(cm), the lens' focal length is set to 15cm, and the wavelength of the simulated light is 0.5 micrometers(μm).

2.2.1 Lens Makers Equation

The equation at the root of this research is the Lens Maker's Equation. When an object is in focus, the Lens Maker's Equation is depicted in Equation 7 which can be

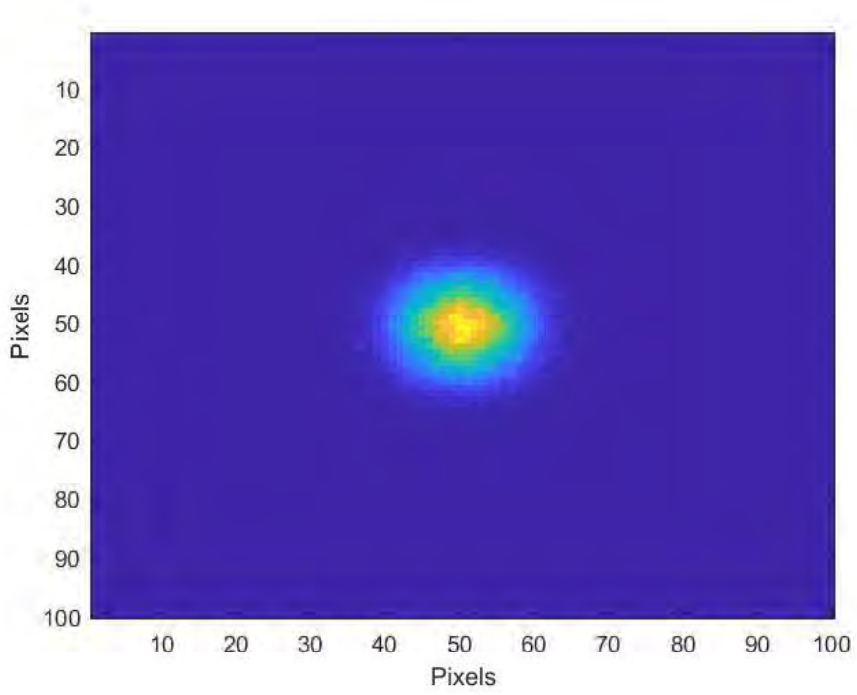

Figure 6: Camera B Output

found in Goodman's Fourier Optics book [4].

$$\frac{1}{z_1} + \frac{1}{z_2} = \frac{1}{f_l} \tag{7}$$

where z_1 is the distance from the lens to the object, z_2 is the distance from the lens to the focal plane, which is generally a known value, and f_l is the focal length of the lens (which is also known). In this research, Equation 7 was more often seen as Equation 8 with a slight modification.

$$\frac{1}{z_1} + \frac{1}{z_2} - \frac{1}{f_l} = C \tag{8}$$

where C is zero if the image is in focus and non-zero if the image is not in focus. In the simulation, two cameras are used and the values for z_1 are set for camera A and camera B (these values were chosen as 3 and 2 meters respectively). After plugging

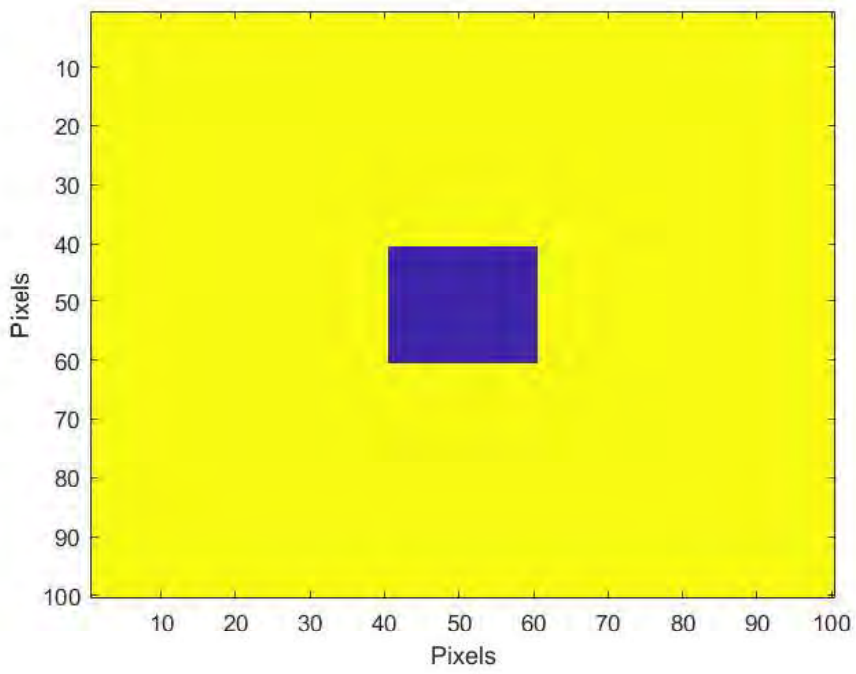

Figure 7: Simulated Range Image

in these values, as well as the focal length, into Equation 8, the values for z_2 can be solved for in the following expressions:

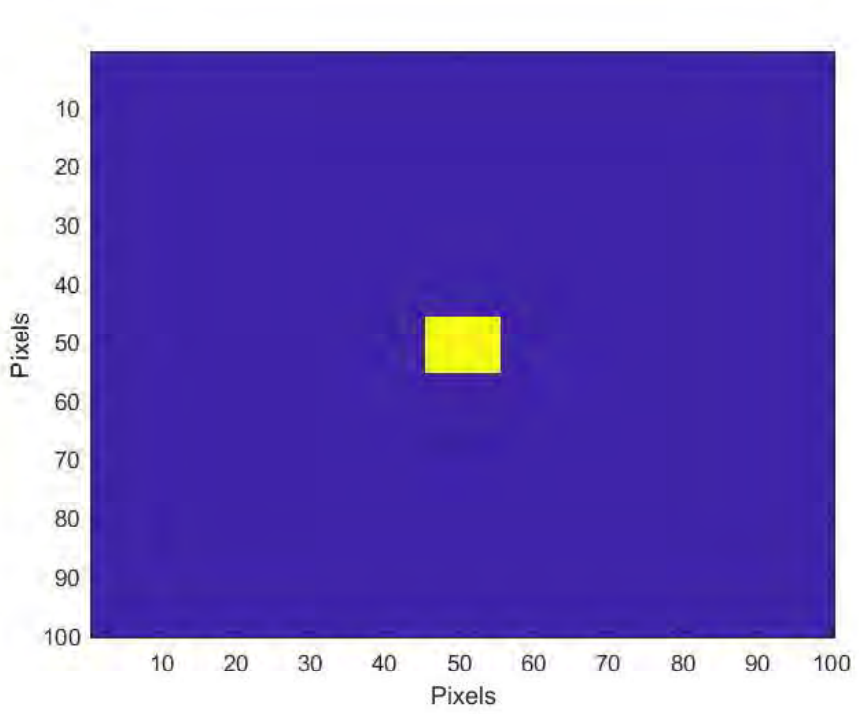

Figure 8: Simulated Reclectivity Image

$$
\begin{aligned}
z_{1A} &= \frac{1}{\frac{1}{0.15} - \frac{1}{2}} \\
&= \frac{1}{6.6667 - .5} \\
&= \frac{1}{6.16667} \\
&\approx 0.1622m \\
z_{1B} &= \frac{1}{\frac{1}{0.15} - \frac{1}{3}} \\
&= \frac{1}{6.6667 - .3333} \\
&= \frac{1}{6.3334} \\
&\approx 0.1579m
\end{aligned}
$$

These values are the distances from the lens to the focal plane of the cameras,

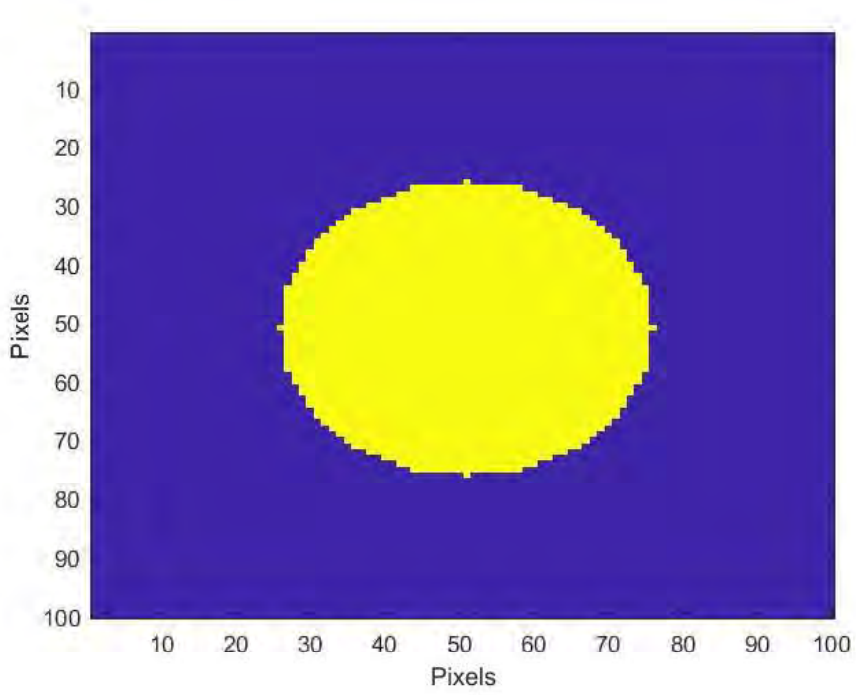

Figure 9: Simulated Aperture Image

where z_{1A} and z_{1B} are for camera A and camera B respectively. In lab, these values would be used to determine how far back to set the camera from the lens. After obtaining all the necessary values, data must be generated for the algorithm.

2.3 Generating Data

In order to generate the required data for the simulation, a PSF must first be simulated. Inside the method that generates the PSF, there are a couple values ($d(x, y)$ and z_2) that are calculated in order to generate the aperture shown in Figure 9. The distance from each pixel is calculated by the using the formula shown in Equation 9.

$$d(x, y) = \sqrt{(x - x_1)^2 - (y - y_1)^2} \tag{9}$$

where $d(x, y)$ is the physical distance, x_1 and y_1 are the center point of the aperture array, and x and y are each individual point in the array. The program passes in a radius and depending on its size, the program places either 1 or 0 to create an image of the aperture. The distances calculated are compared to the radius in order to determine the 1s and 0s. For this simulation, the aperture is shown in Figure 9. The pupil of the simulation must then be calculated. This is done with Equation 10.

$$P(x, y) = A(x, y)\cos(\phi(x, y)) + iA(x, y)\sin(\phi(x, y)) \tag{10}$$

In this equation, $A(x, y)$ is the aperture at any given pixel, which is shown in Figure 9, $P(x, y)$ is the pupil function, and $\phi(x, y)$ is the phase of the light at each pixel, whose calculation is shown in Equation 11.

$$\phi(x, y) = \frac{\pi d^2(x, y)C}{\lambda z_1} \tag{11}$$

The program also passes in a radial size, the focal length of the lens, and the number of pixels in the aperture array. The phase value passed in for the simulation is λ, the wavelength of the light. The PSF, referenced as $h(u, v)$, is then calculated by using Equation 12.

$$h(u, v) = |\mathfrak{F}\{P(x, y)\}|^2 \tag{12}$$

This program outputs the PSF at one location is the output array based on the z_2 values calculated at the beginning of the program. There are two z_2 values to simulate two different cameras, or one camera focusing at two different z values. This program executes a loop to calculate the PSF at all output pixels and then scales the PSF by the reflectivity. This is the non-noisy output image. The output image is then made noisy and the noise takes on a Poisson distribution. Combining everything, the

non-noisy signal is obtained using the Equation 13 [4].

$$i(x_2, y_2) = \sum_u \sum_v Reflect(u, v)h[u, v, x_2, y_2, z_2(u, v)] \tag{13}$$

Once the noise is added to these two images, they are displayed to the user, shown in Figures 5 and 6. These images are the result of the data generation and are ready to be processed through the algorithm.

III. Data Processing

3.1 Preamble

In order to explain how the simulation and lab data obtain their range information, the processing of data and the algorithm used must be explained. Furthermore, results of the algorithm being applied to the simulation data will be shown and error plots from each simulated camera will be illustrated. The connection between the algorithm and simulated data will then be discussed.

3.2 Processing Introduction

After obtaining data, it needs to be analyzed so the range can be computed. This data goes through an algorithm in order to obtain distances from the pictured object. Two PSFs are generated that represent the PSFs from both independent cameras. From there, error is calculated and plotted. The graph of each camera's error plots are analyzed to find each minimum value. These minimums represent the most likely range from the camera to the lens.

3.3 Processing Algorithm

The algorithm starts by estimating the range to be the minimum value input by the user, computes the error between the camera image and the model image at that range, and then moves on to the next estimated range value. For the simulation, 3 meters was used as the max distance to try and simulate the lab table as close as possible. The set of vectors does not have to start at zero. The minimum can be set at any distance the user would like. If the refueling tanker is a known distance away, a window of estimates can be used as the vector of estimate range values. The algorithm then passes these estimates into the program to make the PSF at each

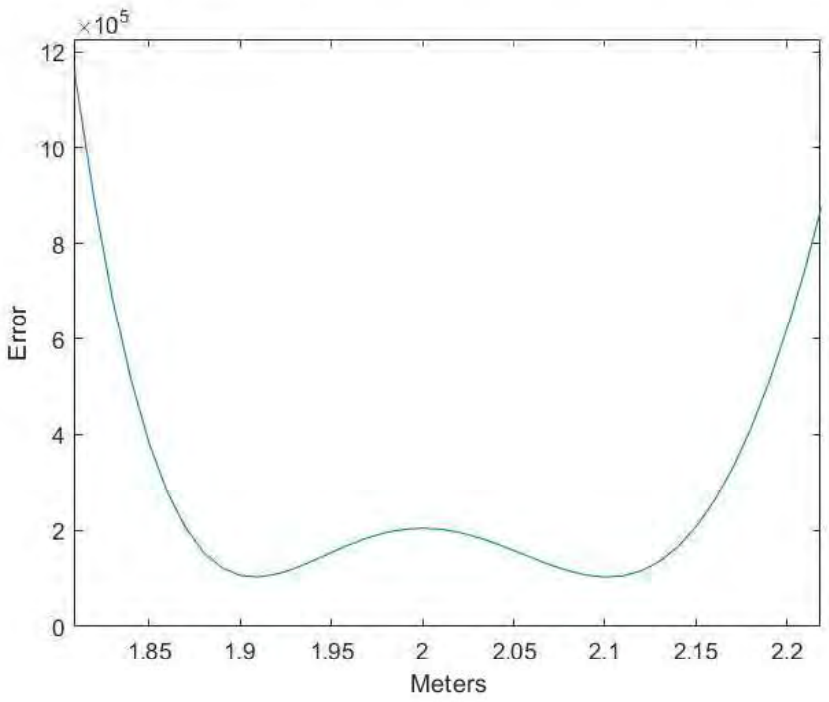

Figure 10: Camera A Error

estimated distance. The Fourier Transform is then taken of the PSF and multiplied by the fast Fourier transform (FFT) of the reflect image to create the convolution of the true image and the PSF. The result of the convolution for each camera are the images $t_a(x, y)$ and $t_b(x, y)$. These images are created by blurring the focused image with the individual PSFs. The error is calculated using Equation 14 for camera A and Equation 15 for camera B. $O(x, y)$ is the simulated data. This matrix is then added to the temporary image for each camera and looped, incrementing z_{1est} by 0.01 meters. Then the error for that point is plotted. The error is calculated using Equation 14 for camera A and Equation 15 for camera B and $t_a(x, y)$ and $t_b(x, y)$ are the temporary images at each point in the respective cameras. Furthermore, $O(x, y)$ is the simulated camera data of the desired object.

$$E_a(z_{1est}) = \sum_x \sum_y (O(x, y) - t_a(x, y))^2 \tag{14}$$

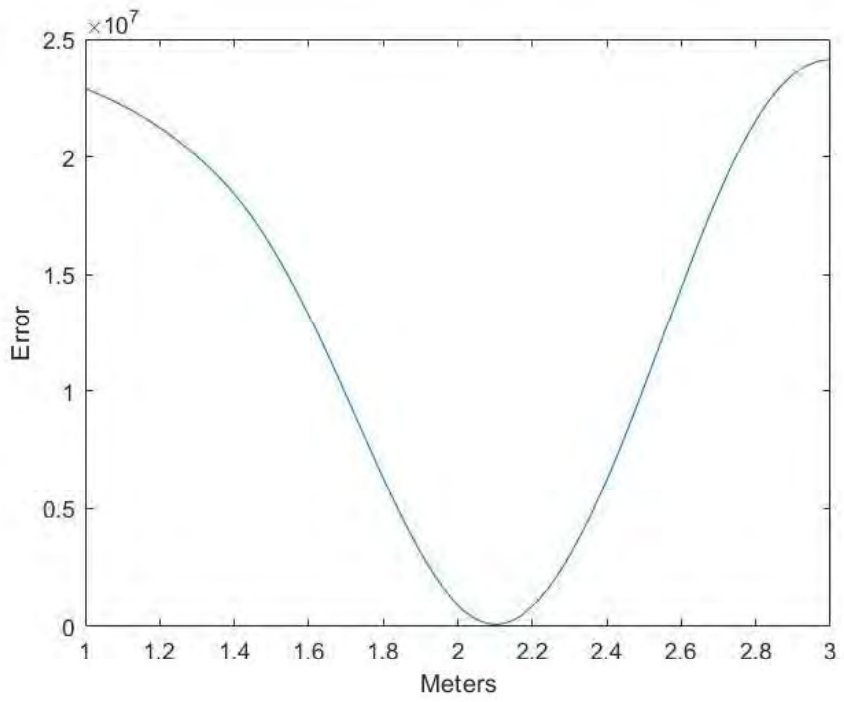

Figure 11: Camera B Error as a Function of Estimated Distance

$$E_b(z_{1est}) = \sum_x \sum_y (O(x,y) - t_b(x,y))^2 \tag{15}$$

While there are several error functions that could have been used, there are some advantages to using the minimum squared error technique. These formulas also assist with eliminating very large, unneeded values from the algorithm. The total error of the system can be calculated from adding the errors from each camera used in the system, as illustrated in Equation 16.

$$E_t(z_{1est}) = E_a(z_{1est}) + E_b(z_{1est}) \tag{16}$$

The loop increments z_{1est} by 0.01 each iteration and the error is calculated and plotted for every z_{1est} value. Each camera has its own data and plot. The data from camera A and camera B each go through this algorithm. The error plot from

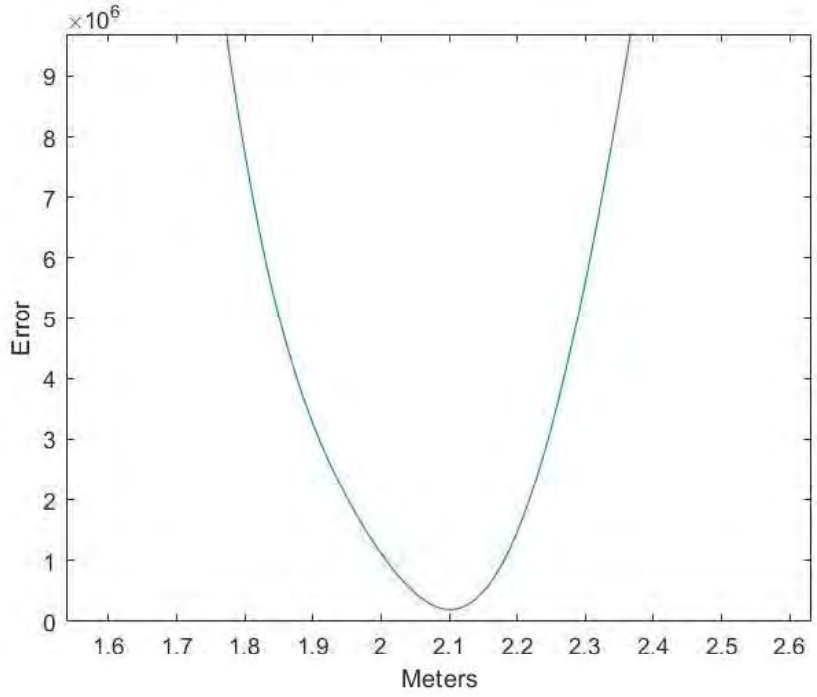

Figure 12: Combined Error as a Function of Estimated Distance

camera A can be seen in Figure 10 while the error plot from camera B can be found in Figure 11. Each error plot shows two minimums due to the object being away from or towards the observer. In Figure 11, there is only one minimum because the second minimum is thought to exist outside of the three meter maximum. There is, however a common minimum to the plots which can be found by adding the two error vectors together in order to obtain the total error of the system. This plot can be seen in Figure 12. The loop starts using the values from Table 1.

The loop from the code to generate the PSFs for these independent error plots can be seen in Figure 13 where Δ is the incrementing value, set to 0.01 for this algorithm. The program starts by setting z_{1est} to z_{min} as its initial value. From there, it creates an initial temporary image for each camera (A and B). The next step is to combine the temporary images($t_a(x, y)$ and $t_b(x, y)$) with the reflect image(from Equation 6) and the A and B channel PSFs. Error is the calculated by use of Equations 14 and

Table 1: Initial Data Processing Values

Variable	**Value**
z_{1est}	1
z_{1max}	3
z_{1a}	2
z_{1b}	3
z_{2a}	0.162
z_{2b}	0.158
ReflectImage	1000
Wavelength(λ)	$0.500\mu m$
Focal Length(f_l)	$0.150cm$
Lens Diameter(D_l)	0.010
True Range(R)	2.500
Number of Pixels(N)	100

15 when compared to the data. From there, the algorithm increments z_{1est} by the 0.01 and checks to see if it equals z_{max}. If z_{1est} equals z_{max}, the algorithm stops and displays the error plots. If they aren't equal, then the algorithm recalculates PSF_a and PSF_b and loops back into recalculating $t_a(x, y)$ and $t_b(x, y)$ for the next loop. For real world applications, the true z_1 can be a positive number close or equal to zero whereas a max value of $z_1(z_{1max})$ can be obtained using the Radio Detection and Ranging (RADAR) system from the aircraft. This system will be able to supply the program with a close enough max range value, although, it won't be exact.

3.3.1 Timing

It is important to see how efficient the algorithm is with data. The program is ran, which includes generating data, running the algorithm, plotting the error, and giving an estimated range calculation to the user. After the program concluded, time measurements were taken throughout the program in order to see how efficient the method was. Table 2 shows the times taken from different areas of the program. The estimated range iteration time is based on one z_{1est} value. The more z_{1est} values

that are used, the more time is needed to complete the program. Another aspect worth noting is that the time is based on the specifications of the computer that the program is ran on. Better specifications can reduce the times drastically.

Table 2: Algorithm Times

Description	**Time**
Variable Declaration	$0.030s$
Estimated Range Iteration	$13s$

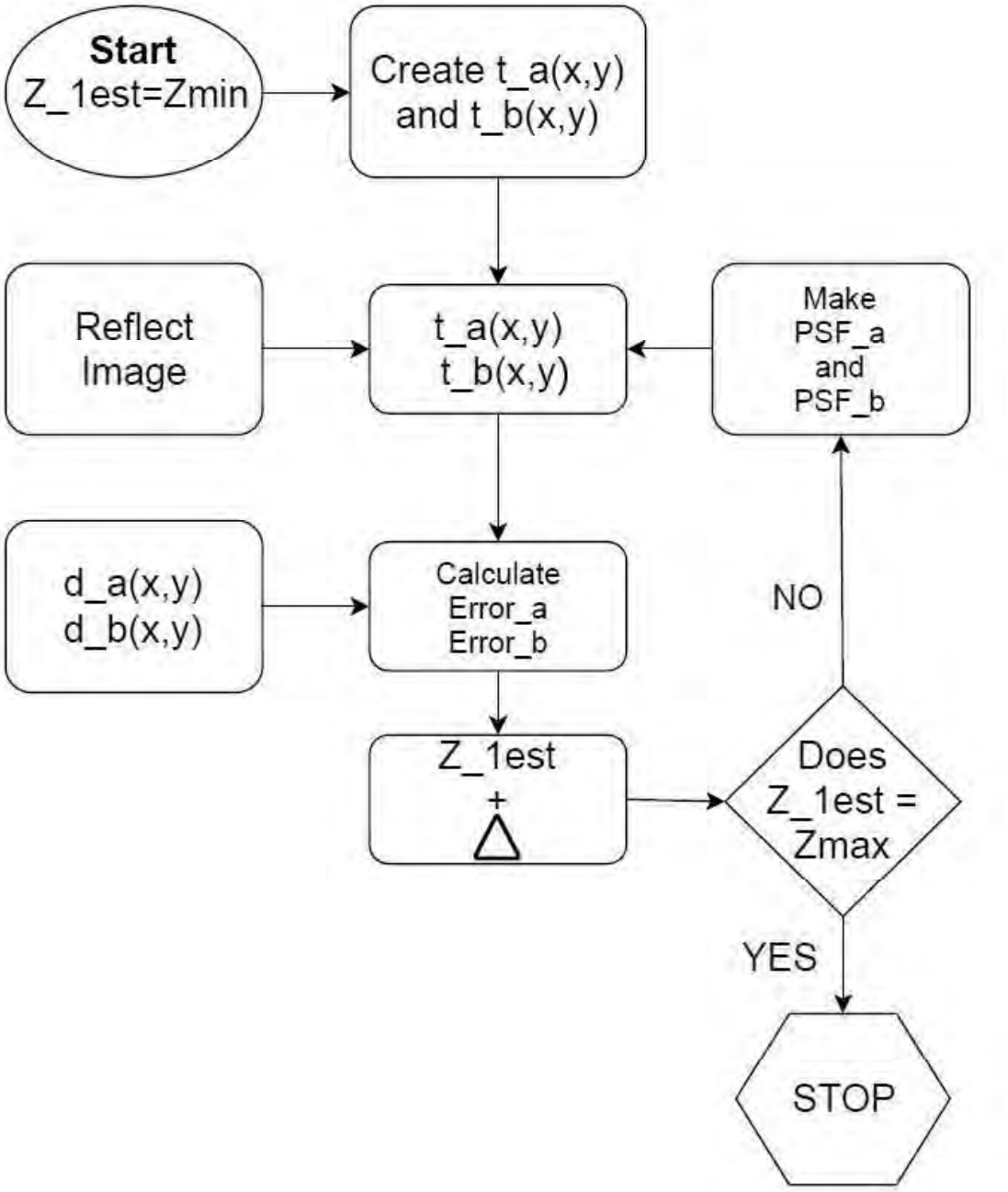

Figure 13: Error Flowchart

IV. Laboratory Data

4.1 Preamble

This chapter will outline the use of the algorithm with data obtained in the lab. It will talk about how the data was captured in the lab specifically, as well as tests used before the algorithm was ran. For the lab data, it was important that the lens whos focal length's error had the lowest variance was used in order to obtain the best error estimate possible. This process will be discussed in the chapter. Also, how the data went from a photograph by a camera to an image that was usable through Matlab.

4.2 Laboratory Introduction

The laboratory setup features placement of a thin lens in front of a camera directed at a lamp with a pinhole aperture in front of it. Furthermore, a red filter is placed between the camera and the main lens. This is because if standard light is used, there is too much intensity for the camera to get a clear photo. By placing the red filter into the system, a clear image is formed. After the setup, the light source is moved until it's in focus to the camera. The distance is measured and a picture is taken. Then, the lens is moved as well as the light source in order to get another clear image. This is to simulate using two cameras due to the lab only containing one. After the images are captured, they are inputted into Matlab in order to be processed through the algorithm. A diagram of how the lab is setup for this experiment is illustrated in Figure 14.

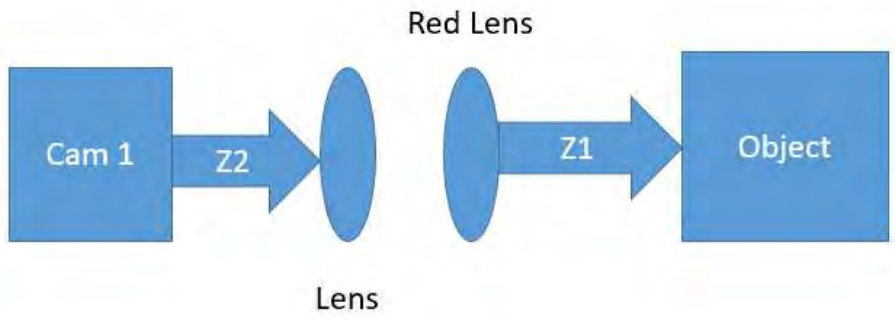

Figure 14: Lab Diagram

4.3 Lens Selection

In order to ensure the correct lens was used, a variance calculation had to be made over many trials of the code. The focal lengths would be cycled through the code based on actual availability in the lab and the lens with the lowest error variance was used in the experiment . The focal lengths were tested over 100 cycles. The variances were recorded and can be seen in Table 3. The lens with the $15cm$ focal length produced the lowest range variance in this simulation and was used for the actual laboratory experiment described in the the next section.

The specifications for the lab experiment are shown in Table 4 and these values did not change throughout the experiment.

Table 3: Focal Length of Lenses

Focal Length of Lens	**Variance**
10 cm	$0.118m^2$
15 cm	$0.107m^2$
175 mm	$0.116m^2$
20 cm	$0.110m^2$

Table 4: Initial Lab Values

Variable	**Value**
Number of Pixels (N)	250
Background Light (Camera A)	83 digital counts
Background Light (Camera B)	160 digital counts
Diameter of Lens(D_{lens})	$0.150m$
Wavelength(λ)	$0.600\mu m$
z_{1A}	$1.854m$
z_{1B}	$1.702m$
z_{2A}	$0.106m$
z_{2B}	$0.106m$

4.4 Lab Results

The main difference between the lab and simulation is that the data is not simulated. The data is captured images from the lab. This allows for faster processing speeds of the program overall. The images were cut down to the size needed to see the entire image. There were 4 images needed. Two from different ranges to simulate two different cameras and each of them being in and out of focus. These images are shown in Figures 15, 16, 17, and 18. For this program to work, the in-focus image had to line up exactly with the out of focus image. In order to accomplish this, the correlation between the in focus and out of focus image was taken. Then, the max value in both dimensions was found and each image was shifted by using Equations 17 and 18 where N is the number of pixels in each dimension. In these equations, X_{shift} is the amount of shift that an image needs to be shifted for it to line up with the true image horizontally while Y_{shift} performs the same function, but vertically. X_{max} and Y_{max} refer to the maximum values, by intensity of the images.

$$X_{shift} = X_{max} - \frac{N}{2} \tag{17}$$

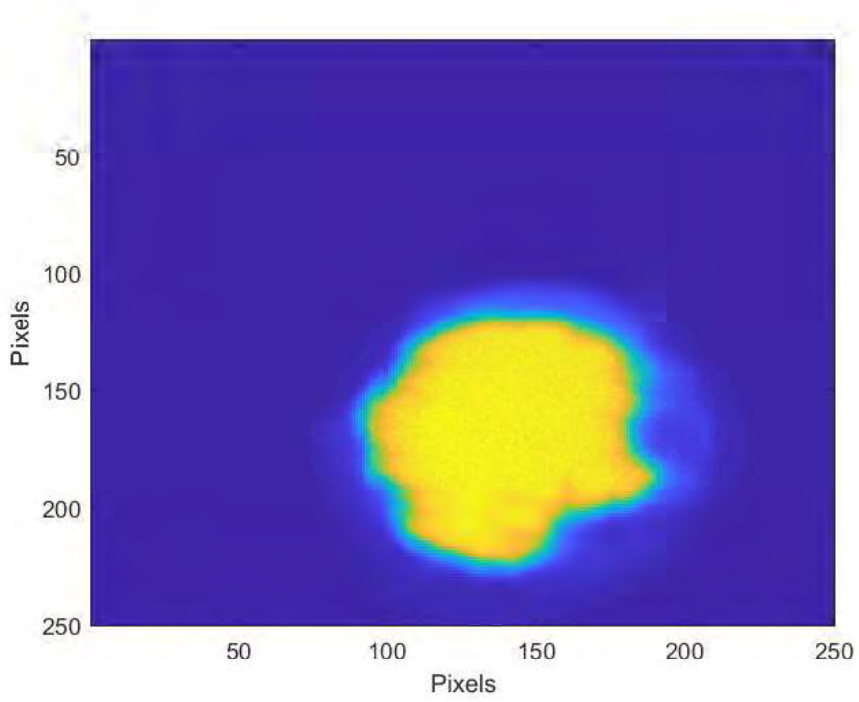

Figure 15: Camera A In Focus Image

$$Y_{shift} = Y_{max} - \frac{N}{2} \tag{18}$$

The images from each camera (A and B) use Equations 17 and 18 to shift their respected images the amount needed in order to be analyzed.

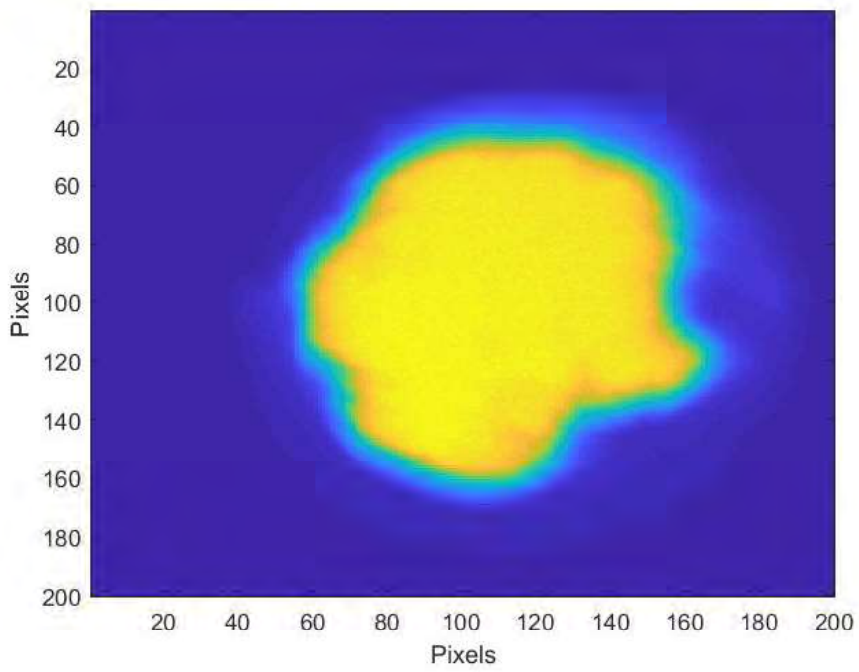

Figure 16: Camera B In Focus Image

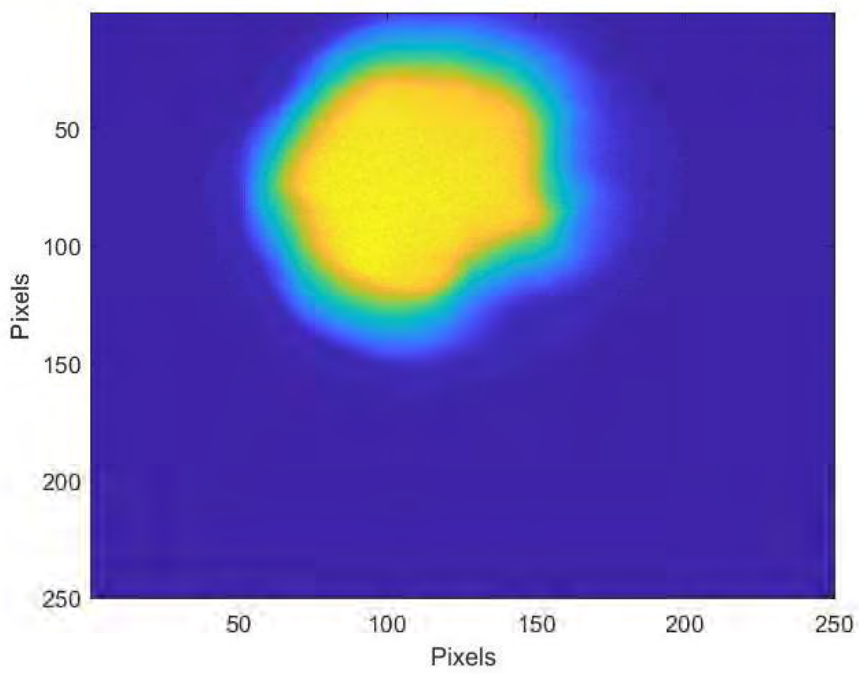

Figure 17: Camera A Out of Focus Image

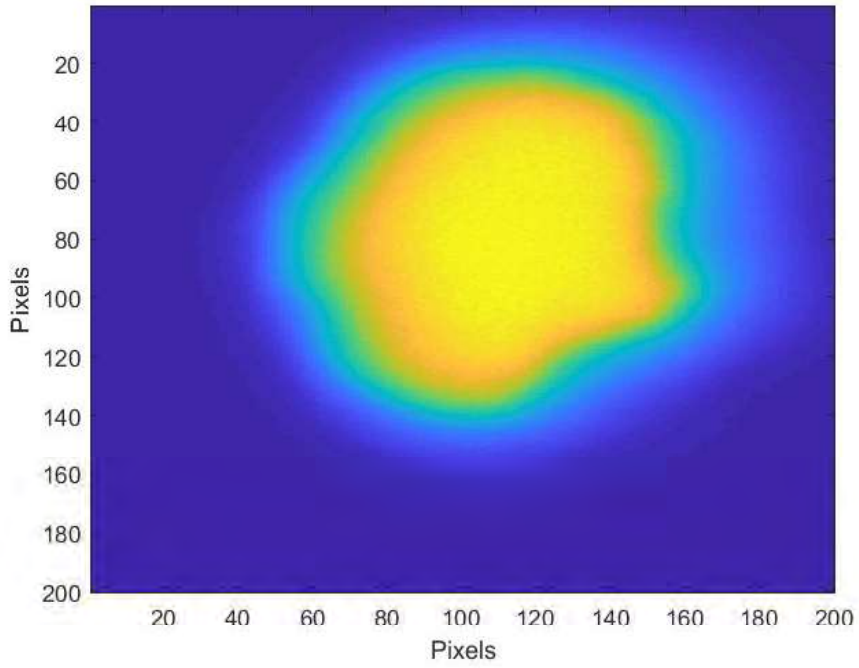

Figure 18: Camera B Out of Focus Image

4.5 Image Alignment

As mentioned in Section 4.4, the images must line up perfectly in order to be processed through the algorithm. The non-shifted image pairs are seen in Figures 15 and 17 for camera A and Figures 16 and 18 for camera B. After using Equations 17 and 18, the images can be shifted to line up with each other. The resulting, shifted image from camera A is shown in Figure 19 and Figure 20 for camera B. When compared to the output images from each camera, it's easily seen that the images align perfectly and are ready to be processed through the algorithm. From the program, the true range is 73 inches(1.85 meters) and the estimated range is outputted as 1.9 meters. Using Equation 19, the percent error from the true range can be found.

$$E = \frac{|R_{est} - R_{true}|}{R_{true}} * 100 \tag{19}$$

where R_{est} is the outputted estimated range, and R_{true} is the known true range. After plugging in the values for these variables, the program obtains a percent error of 2.7%. Figures 21 and 22 show the error plots associated with each camera. There are not always two different errors within the range estimates but the process of obtaining the true range stays the same in case there are two. Nevertheless, if there are two in each image, there will be one common error point (or close to each other) between the two plots. This is the program's estimated range value.

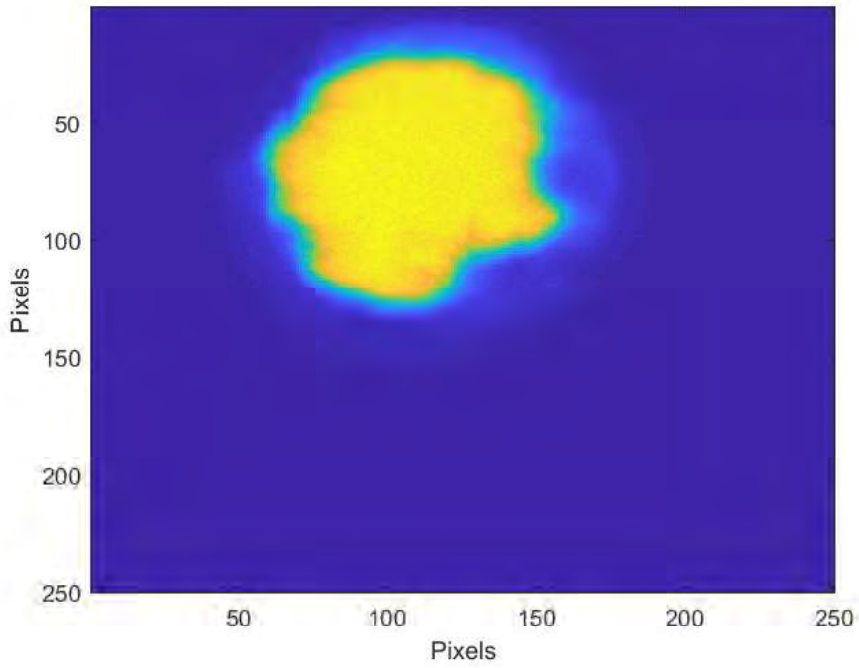

Figure 19: Camera A Aligned Image

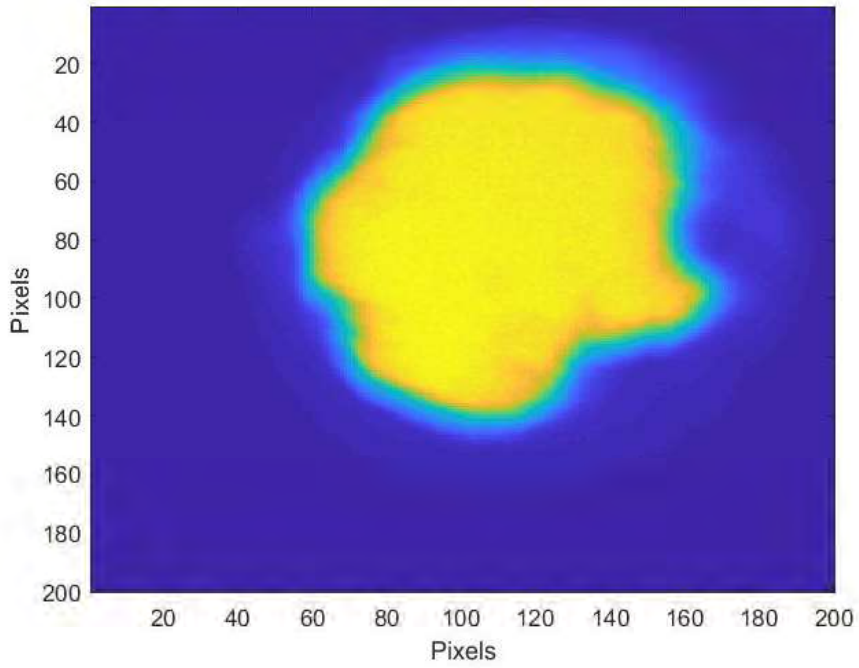

Figure 20: Camera B Aligned Image

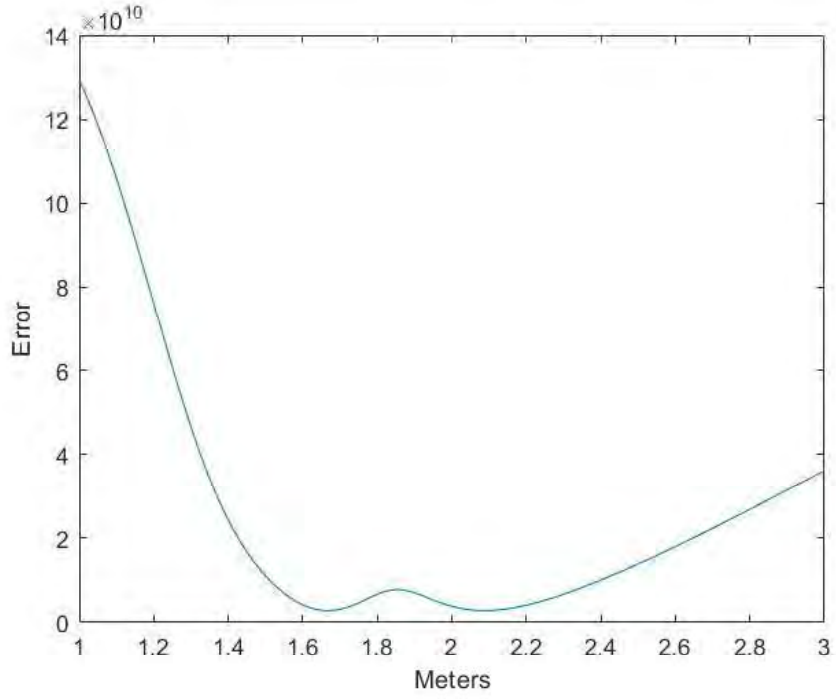

Figure 21: Error from Camera A

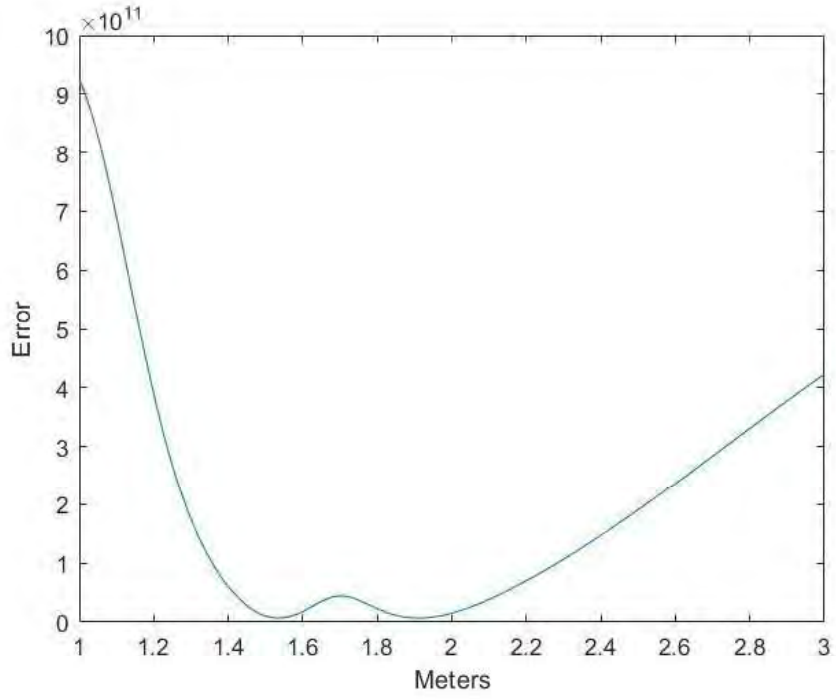

Figure 22: Error from Camera B

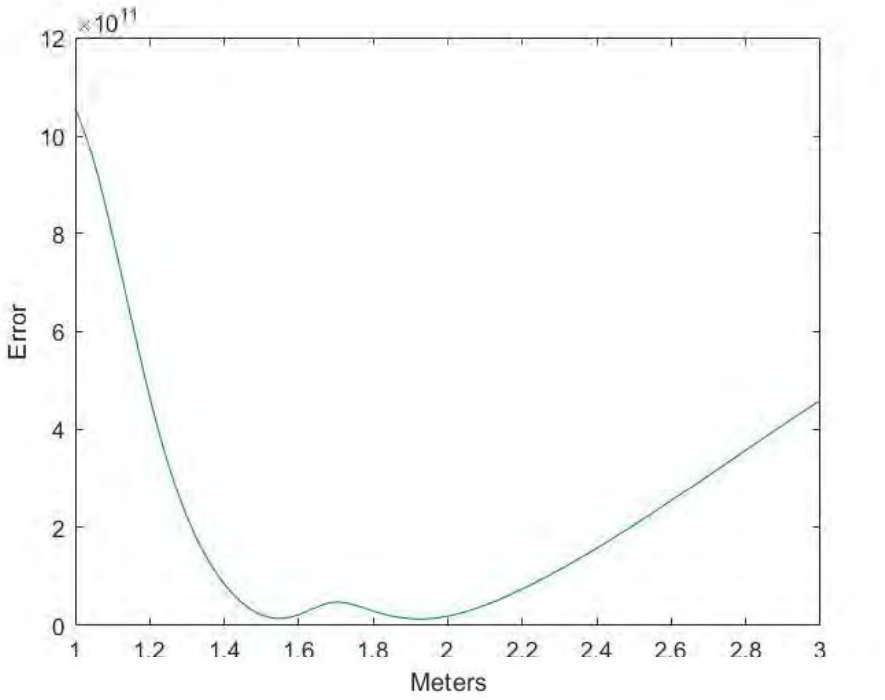

Figure 23: Overall Lab Error

V. Conclusions

Extracting range data can be an extremely daunting task and there are many different factors that play a roll when using methods which are already heavily researched, mainly stereo cameras. With stereo cameras, the system needs to have the cameras not too close together in order to obtain accurate range estimates. When using focus error to extract range data, the cameras can be as close together as need be. With closer cameras, pitch of the aircraft may becomes less of an issue. This is because if the cameras are essentially touching each other, no matter what the position of the aircraft, the image taken will basically be the same.

This research pinpointed the need for more efficiency of gathering range data with the focus error method having roughly 8% error in simulation. The algorithm is fairly simplistic, processing the data doesn't take too much time, and all within a reasonable error rating as shown by the simulated test results.

Looking forward, efficiency is still an aspect that can be researched further. Creating a way that could combine the use of stereo cameras and focus error to find range data would be a major contribution. A good starting point could be analyzing different distances with stereo cameras relating to each other and then applying the focus error method to each camera.

Processing time would also be a key aspect that could be improved. With this research being fairly new, efficiency was not a huge priority. Data processing could be faster, leading to more results. This can directly improve accuracy and minimize the error in the system. Implementing the use of a single camera could be a huge benefit to the overall efficiency of the system as well. Reviewing the future work, here's a list of what improvements can be made:

- Improve efficiency of the overall program

- Improve error rating
- Combining stereo cameras and focus error
- Decrease processing time
- Conduct more lab trials so the real world accuracy of the algorithm can be established

Bibliography

1. Rebecca Grant. Refueling the RPAs.

2. J. C. Rodríguez-Quiñonez, O. Sergiyenko, W. Flores-Fuentes, M. Rivas-lopez, D. Hernandez-Balbuena, R. Rascón, and P. Mercorelli. Improve a 3D distance measurement accuracy in stereo vision systems using optimization methods' approach. *Opto-electronics Review*, 25(1):24–32, may 2017.

3. Ba Nguyen Steve McLaughlin, Mark Pilling, Phillip "PD" Weber. Standardizing Automated In-Air Refuelinig. 2019.

4. Joseph Goodman. *Introduction to Fourier Optics*. McGraw-Hill Higher Education, New York City, 2nd editio edition, 1996.

Acronyms

A3R automated air-to-air refueling. iv, 1, 7

AAR air-to-air refueling. iv, 6

AFRL Air Force Research Laboratory. 4

DARPA Defense Advanced Research Projects Administration. 3

FFT fast Fourier transform. 19

GPS global positioning system. 3

NASA National Aeronautics and Space Administration. 3

PSF point spread function. 10, 15, 16, 18, 19, 21

RPA remotely piloted aircraft. 5

UAV unmanned aerial vehicle. 1, 3

REPORT DOCUMENTATION PAGE

Form Approved
OMB No. 0704-0188

PLEASE DO NOT RETURN YOUR FORM TO THE ABOVE ADDRESS.

1. REPORT DATE *(DD-MM-YYYY)*	2. REPORT TYPE	3. DATES COVERED *(From - To)*
26-03-2020	Master's Thesis	Oct 2018-Mar 2020

4. TITLE AND SUBTITLE

Extracting Range Data from Images using Focus Error

5a. CONTRACT NUMBER

5b. GRANT NUMBER

5c. PROGRAM ELEMENT NUMBER

6. AUTHOR(S)

Madden, Erik M, 2d Lt

5d. PROJECT NUMBER

5e. TASK NUMBER

5f. WORK UNIT NUMBER

7. PERFORMING ORGANIZATION NAME(S) AND ADDRESS(ES)

Air Force Institute of Technology
Graduate School of Engineering and Management (AFIT/EN)
2950 Hobson Way
Wright-Patterson AFB OH 45433-7765

8. PERFORMING ORGANIZATION REPORT NUMBER

AFIT-ENG-MS-20-M-037

9. SPONSORING/MONITORING AGENCY NAME(S) AND ADDRESS(ES)

Colonel Bryan Neff
Department Head, Electrical and Computer Engineering
Air Force Academy
2304 Cadet Drive, Suite 3100
USAF Academy, CO 80840-5002

10. SPONSOR/MONITOR'S ACRONYM(S)

USAFA

11. SPONSOR/MONITOR'S REPORT NUMBER(S)

12. DISTRIBUTION/AVAILABILITY STATEMENT

Distribution Statement A. Approved for public release; Distribution Unlimited

13. SUPPLEMENTARY NOTES

14. ABSTRACT

Air-to-air refueling (AAR) has become a staple when performing long missions with aircraft. With modern technology, however, people have began to research how to perform this task autonomously. Automated air-to-air refueling (A3R) is this exact concept. Combining many different systems, the idea is to allow computers on the aircraft to link up via the refueling boom, refuel, and detach before resuming pilot control. This document lays out one of the systems that is needed to perform A3R, namely, the system that extracts range data. While there are stereo cameras that perform such tasks, there are difficulties that play a role due to stereo cameras needing distance between themselves. This research uses focus error to extract the range from an image and can eliminate some potential errors that surface when using stereo cameras. This document will discuss how far A3R has come, the benefits of a focus error method, a simulation of how this process can function, to include a processing algorithm, as well as a laboratory section, which also describes all results and improvements that can be made in the future.

15. SUBJECT TERMS

Range Estimation, Focus Error, Automated Refueling

16. SECURITY CLASSIFICATION OF:			17. LIMITATION OF ABSTRACT	18. NUMBER OF PAGES	19a. NAME OF RESPONSIBLE PERSON
a. REPORT	b. ABSTRACT	c. THIS PAGE			Dr. Stephen C Cain, AFIT/ENG
U	U	U	UU	49	19b. TELEPHONE NUMBER *(Include area code)* (937) 255-3636 x4716 stephen.cain@afit.edu